Correlated Electron-Hole Transitions in Bulk GaAs and GaAs-(Ga,Al)As Quantum Wells: Effects of Applied Electric and In-Plane Magnetic Fields

C. A. Duque[1], L. E. Oliveira[2], and M. de Dios-Leyva[3]
[1]*Instituto de Física, Universidad de Antioquia, AA 1226, Medellín, Colombia*
[2]*Instituto de Física, Unicamp, CP 6165, Campinas-SP, 13083-970, Brazil*
[3]*Dept. of Theor. Physics, Univ. of Havana, San Lázaro y L, Vedado 10400, Havana, Cuba*

Received on 8 December, 2005

The effects of crossed electric and magnetic fields on the electronic and exciton properties in semiconductor heterostructures have been investigated within the effective-mass and parabolic band approximations for both bulk GaAs and GaAs-$Ga_{1-x}Al_xAs$ quantum wells. The combined effects on the heterostructure properties of the applied crossed electric/magnetic fields together with the direct coupling between the exciton center of mass and internal exciton motions may be dealt with via a simple parameter representing the distance between the electron and hole magnetic parabolas. Calculations lead to the expected behavior for the exciton dispersion in a wide range of the crossed electric/magnetic fields, and present theoretical results are found in good agreement with available experimental measurements.

Keywords: Quantum well; Magnetic field; Electric field; Exciton transitions

A detailed knowledge of the optical properties of semiconductor heterostructures is of paramount importance for possible device applications. In that respect, the study of exciton properties in those systems is of great interest as such coupled electron-hole ($e-h$) excitations, which arise from the $e-h$ Coulomb interaction, may considerably modify the interband optoelectronic properties of semiconductor heterostrutures. When the electron and hole carriers are confined in the same region of the direct space and in the same point of the inverse k-space, the exciton is called a direct exciton; alternatively, if the carriers are confined in different regions of the direct space and/or in different points of the inverse k-space the exciton is termed as an indirect exciton. Work on exciton properties have been recently performed both experimentally [1–4] and theoretically [5–12]. Luminescence measurements in GaAs-$Ga_{1-x}Al_xAs$ double quantum wells (QWs) under in-plane magnetic fields [1, 2] have concluded that the dominating radiative recombination of localized indirect excitons does not allow one to observe the quenching of the spatially indirect exciton luminescence and the quadratic shift of their energy under in-plane magnetic fields, with the consequence that the possibility of an exciton dispersion engineering would then be limited in these kinds of samples.

Combined theoretical and experimental studies from Ashkinadze *et al* [11] for the effect of an in-plane magnetic field on the photoluminescence (PL) spectrum of modulation-doped heterostructures have suggested that there are remarkable spectral modifications of the PL spectra in both modulation-doped QWs and high-quality heterojunctions, due to $B_{\|}$-induced modifications in the direct optical transitions in QWs, and effects on the free holes in heterojunctions, respectively. Also, studies [12] on the magnetic-field effects on indirect excitons in coupled GaAs-(Ga,Al)As QWs reveal that the exciton effective mass is enhanced as the growth-direction magnetic field increases and, at high fields, it becomes larger than the sum of the e and h masses, suggesting that a magnetoexciton is an excitation with effective mass determined by the coupling [5] between the exciton center of mass (CM) motion and internal structure rather than by the masses of its constituents. A recent theoretical calculation [12] suggest that the inclusion of both the effects of the finite-width barrier and well confining potentials as well as of the appropriate electronic band structure could be important for a realistic description of experimental results.

The aim of the present work is to study the magneto-Stark effect for confined excitons in single GaAs-$Ga_{1-x}Al_xAs$ QWs. The magnetic field B is taken as perpendicular to the growth direction of the heterostructure, whereas the applied electric field E is along the z-growth direction. Here, for simplicity, we will work within the effective-mass and nondegenerate-parabolic band approximations. The Hamiltonian for the exciton may be written as

$$\hat{H} = \sum_{i=e,h} \left[\frac{1}{2m_i^*} \left(\hat{\vec{p}}_i - \frac{q}{c}\vec{A}_i \right)^2 + V_i(z_i) \right] - \frac{e^2}{\varepsilon|\vec{r}|} + e\vec{E}\cdot\vec{r}, \quad (1)$$

where e and h stands for electron and hole, respectively, $\vec{A}_i = \vec{A}(\vec{r}_i)$ are the vector potentials associated to the magnetic field, $\hat{\vec{p}}_i$ and m_i^* are momentum operators and effective masses, respectively, the V_i are the confining potentials, $q = -e$ for electrons and $+e$ for holes, where e is the absolute value of the electron charge, ε is the dielectric constant, and $\vec{r} = \vec{r}_e - \vec{r}_h$ is the relative electron-hole position. The above mentioned parameters for bulk GaAs and $Ga_{1-x}Al_xAs$ barrier were taken at low temperatures from the data collected by Li [13]. For the dielectric constants and electron and heavy-hole effective masses, we have considered the same values as in GaAs throughout the heterostructure [14].

As the heterostructure is grown along the z direction, the Schrödinger equation with the above Hamiltonian is invariant under simultaneous translation of both the e and h coordinates parallel to the (x,y) plane and the corresponding gauge transformation, which leads to the conservation of the $\hat{\vec{P}} = (\hat{P}_x, \hat{P}_y)$ transverse components of the exciton CM magnetic momentum [5, 12]. By choosing the in-plane applied magnetic field along the x direction, $\vec{B} = B\hat{x}$, using the Landau

gauge $\vec{A}(\vec{r}) = -zB\hat{y}$, and a crossed electric field in the growth direction, $\vec{E} = -E\hat{z}$, one may write the common eigenfunctions of both $\hat{H}$ and $\hat{\vec{P}}$ as

$$\Psi_{exc}(\vec{r}_e,\vec{r}_h) \propto \exp\left(\frac{i}{\hbar}\vec{P}\cdot\vec{R}\right)\Phi(\vec{\rho},z_e,z_h)\,, \qquad (2)$$

where $\vec{R}$ is the in-plane exciton CM coordinate, $\vec{\rho}$ is the in-plane internal exciton coordinate, and $\Phi(\vec{\rho},z_e,z_h)$ is the eigenfunction of

$$\hat{H} = \hat{H}_0 - \frac{e^2}{\varepsilon|\vec{r}_e-\vec{r}_h|}\,, \qquad (3)$$

where, by considering the translational invariance in the (x,y) plane,

$$\hat{H}_0 = \frac{P_x^2}{2M} + \frac{p_x^2}{2\mu} - K_y l_B\,(Fl_B) - \frac{(Fl_B)^2}{2\beta_0} + \sum_{i=e,h}\left[\frac{\hat{p}_{iz}^2}{2m_i^*} + V_i(z_i) + \frac{1}{2}m_i^*\omega_i^2\left(z_i - z_i^0\right)^2\right], \qquad (4)$$

with $F = eE$, and eigenvalue

$$E_0 = \frac{P_x^2}{2M} + \frac{p_x^2}{2\mu} - K_y l_B\,(Fl_B) - \frac{(Fl_B)^2}{2\beta_0} + E_\eta^e\left(z_e^0\right) + E_\alpha^h\left(z_h^0\right), \qquad (5)$$

where $\eta,\alpha = 0,1,2,3...$ are the Landau magnetic subband indices, $\beta_0 = \frac{\hbar^2}{Ml_B^2}$, $l_B = \sqrt{\frac{\hbar c}{eB}}$ is the Landau magnetic length (or cyclotron radius), μ is the $e-h$ reduced mass, $z_{e,h}^0$ are the non-correlated e and h orbit-center positions along the growth direction, and $\omega_{e,h}$ are the corresponding cyclotron frequencies. Note that

$$\Delta = z_e^0 - z_h^0 = l_B\left(K_y l_B + \frac{Fl_B}{\beta_0}\right) \qquad (6)$$

represents the spatial distance between the centers of the non-correlated electron and hole magnetic parabolas [5]. The above result for the non-correlated $e-h$ pair allows one to obtain the ground-state exciton energy via a variational procedure with a hydrogenic-like 1s-like type of trial envelope exciton wave function. Details of the calculations will be published elsewhere [15].

We will first present the theoretical results for bulk GaAs. Fig. 1 displays the heavy-hole exciton binding energy E_b, the $e-h$ overlap integral $I_{\rm overlap}$, and the average $e-h$ distance $\langle z_e - z_h\rangle$ along the growth direction. As one can see from Fig. 1(a) and 1(d), the exciton binding energy is a decreasing function of both Δ and E, for each value of B. These results may be understood as follows: As in the bulk the non-correlated electron and hole oscillate around the points z_e^0 and z_h^0, respectively, and the binding energy is determined by the $e-h$ attractive Coulomb interaction, which tends to zero with the $e-h$ distance, it is obvious that E_b must diminish with increasing Δ and applied electric field $E \sim B^2\Delta$ [see eq. (6)

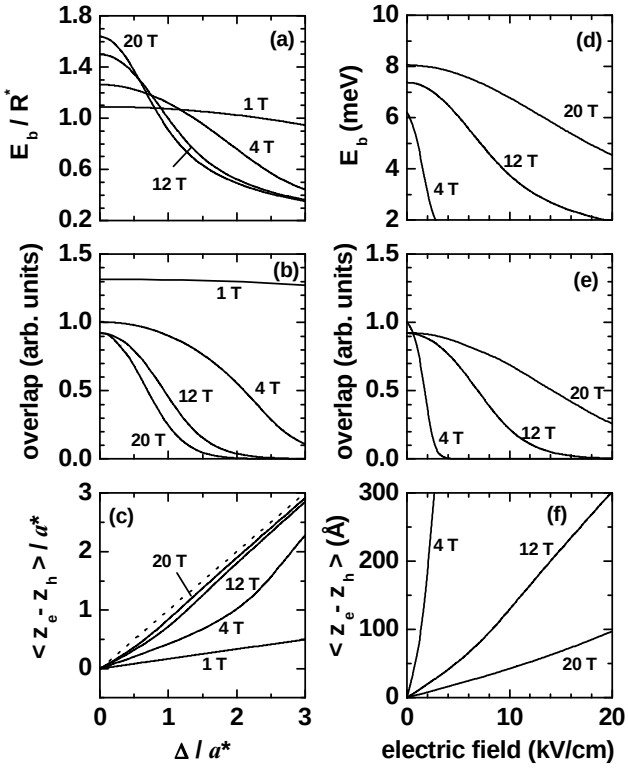

FIG. 1: The heavy-hole E_b exciton binding energies [(a) and (d)], the overlap integral $I_{overlap}$ [(b) and (e)], and the average $e-h$ distance $< z_e - z_h >$ along the growth direction [(c) and (f)] in the z-direction (which is the direction of the applied electric field), for bulk GaAs, K_y = 0, and for various values of the applied in-plane magnetic field, as functions of the spatial distance Δ/a^* between the centers of the electron and heavy-hole magnetic parabolas [(a), (b) and (c)] or as functions of the growth-direction applied electric field [(d), (e) and (f)]. In (c), distances $< z_e - z_h >$ and Δ are given in units of the exciton effective Bohr radius ($a^* = 118$ Å), and energies in (a) are in units of the heavy-hole exciton Rydberg ($R^* = 4.9$ meV). The dashed line in (c) corresponds to the representation of $< z_e - z_h >= \Delta$.

with $K_y = 0$], for a fixed value of the magnetic field. As expected [16], the present calculations for $\Delta = 0$ and $E = 0$ show an increase in the exciton binding energy with increasing values of the magnetic field, i.e., with increasing confinement associated to the magnetic field. Note in Fig. 1(a) that E_b decreases with increasing values of the magnetic field for relatively high (fixed) value of Δ. This behavior is due to the increasing confinement of the electron and hole around their corresponding equilibrium positions as the magnetic field increases, for a given value of Δ. The $e-h$ overlap integral as a function of Δ and of the growth-direction applied electric field $E \sim B^2\Delta$ (when $K_y = 0$) is shown in Figs. 1(b) and 1(e), respectively, for various values of the applied in-plane magnetic field. The rapid decrease of $I_{\rm overlap}$ with Δ and E observed in each curve of Figs. 1(b) and 1(e) is due to fact that the $e-h$ distance in the z-direction increases with Δ. Results for the calculated $\langle z_e - z_h\rangle$ average $e-h$ distance in the z-direction [Figs. 1(c) and 1(f)] are as follows: As shown, $\langle z_e - z_h\rangle = 0$ for $\Delta = 0$ and $E = 0$ for a finite value of the magnetic field,

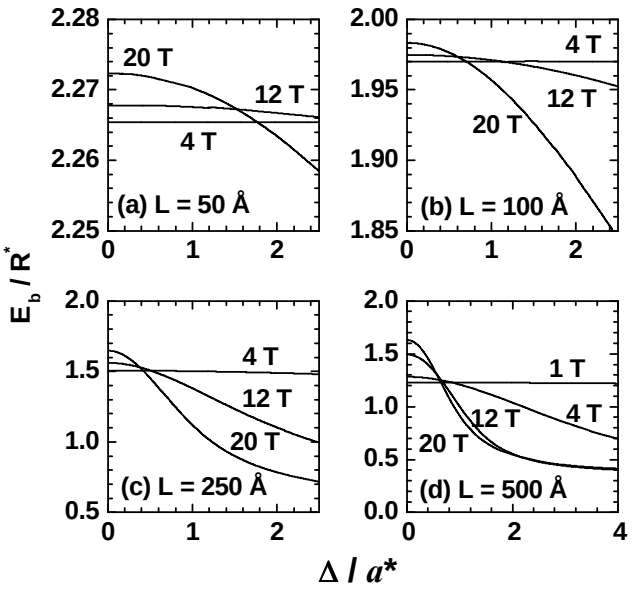

FIG. 2: Heavy-hole exciton binding energy, in units of the heavy-hole exciton Rydberg $R^* = 4.9$ meV, as a function of the spatial distance Δ/a^* ($a^* = 118$ Å is the heavy-hole exciton effective Bohr radius) between the centers of the electron and heavy-hole magnetic parabolas, for GaAs-$Ga_{0.7}Al_{0.3}As$ QWs of different L well widths, and for various values of the in-plane magnetic field. The values of the corresponding growth-direction applied electric field and exciton K_y CM momentum are related to Δ and B via eq. (6).

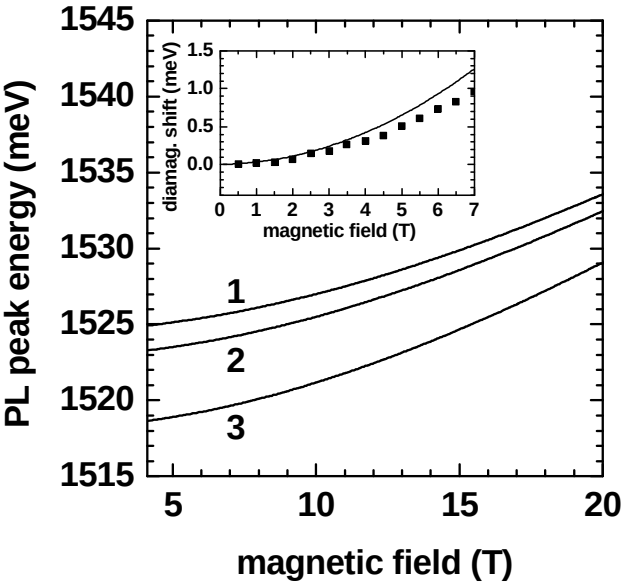

FIG. 3: PL peak energy (or correlated $e-h$ energy transition) for an L = 200 Å GaAs-$Ga_{0.7}Al_{0.3}As$ QW, as a function of the in-plane applied magnetic field, for $K_y = 0$, and different values of the growth-direction applied electric fields (1: E = 0; 2: E = 10 kV/cm; 3: E = 20 kV/cm). The inset shows the diamagnetic shift for the same QW in the absence of the applied electric field (E = 0), compared with the experimental measurements by Ashkinadze *et al* [11].

which may be traced back to the even symmetries of the z-functions involved in the calculations of $\langle z_e - z_h \rangle$. Note that, as z_e^0 and z_h^0 are, respectively, the oscillation centers of the non-correlated electron and hole in the bulk, it is obvious that $\langle z_e - z_h \rangle = z_e^0 - z_h^0 = \Delta$ for the non-correlated $e-h$ pair, and $\langle z_e - z_h \rangle < \Delta$ [see full curves in Figs. 1(c) and 1(f)] for the correlated pair due to the fact that the Coulomb force between the electron and the hole is attractive. Second, because this force tends to zero as $\Delta \to \infty$, it is evident that $\langle z_e - z_h \rangle \to \Delta$ in the limit of high Δ [see full curves in Fig. 1(c)]. As shown in Fig. 1(f), $\langle z_e - z_h \rangle$ increases with E, for a given value of B, because Δ increases with the growth-direction applied electric field. As also shown in Fig. 1(f), $\langle z_e - z_h \rangle$ is a decreasing function for increasing values of B, for a fixed value of the electric field, as Δ decreases with increasing values of the magnetic field.

Figure 2, for GaAs-$Ga_{0.7}Al_{0.3}As$ QWs of different L well widths, shows the present results on the exciton states in the presence of an externally applied growth-direction electric (E) and in-plane magnetic (B) fields. Results are for the heavy-hole exciton binding energy as a function of the spatial distance (Δ) between the centers of the electron and heavy-hole magnetic parabolas, for GaAs-$Ga_{0.7}Al_{0.3}As$ QWs of different well widths (L), and for various values of the applied magnetic field. As the fundamental purpose of our discussion is to study the QW barrier-potential effects on the Δ-dependence of the E_b exciton binding energy, we first note that the results depicted in Fig. 2(d), for an $L = 500$ Å GaAs-$Ga_{0.7}Al_{0.3}As$ QW, are essentially the same as those displayed in Fig. 1(a) for bulk GaAs. This is the result expected for finite values of Δ and sufficiently wide QWs. Another expected result, clearly seen in Figs. 2(a), (b), and (c), is the increase of E_b as L decreases. Also, one should notice that as the QW width decreases, the E_b exciton binding energy tends progressively towards a slow-varying function of Δ, so that it becomes essentially flat for $L = 50$ Å and for the lowest magnetic fields considered [in which case $l_B >> L/2$; see Fig. 2(a)]. This result may be understood if one takes into account that for $l_B >> L/2$ and $z_{h,m}^0 = z_{e,m}^0 - \Delta$ localized inside the QW, the effect of the magnetic field is weak and the exciton binding-energy structure is essentially dominated by the barrier confining potential.

In Figure 3, we present our results for the PL peak energy for an L = 200 Å GaAs-$Ga_{0.7}Al_{0.3}As$ QW, as a function of the in-plane applied magnetic field, for $K_y = 0$, and different values of the growth-direction applied electric fields, i.e.,

$$E_{\rm PL} = E_g - \frac{(Fl_B)^2}{2\beta_0} + E^e_{\eta=0}\left(z_e^0\right) + E^h_{\alpha=0}\left(z_h^0\right) - E_b, \qquad (7)$$

where E_b corresponds to the GaAs band-gap energy. For a fixed value of B (see the different curves in Fig. 3) and increasing values of the applied electric field, one has a decrease in the $e-h$ binding energy as the polarization of the $e-h$ wave function increases, and a decrease in the energies of the $e-h$ non-correlated pair. These two effects lead to a blue-shift or a red-shift, respectively, of the PL peak energy. As the width of the GaAs-$Ga_{0.7}Al_{0.3}As$ QW is quite large (L = 200 Å) the decrease in the energies of the $e-h$ non-correlated pair (under growth-direction applied electric fields) is clearly

the dominant effect, and one should obtain a red-shift effect on the PL peak for fixed values of the magnetic field and increasing strengths of the applied electric field. On the other hand, for a fixed value of the growth-direction electric field, increasing confining effects with increasing values of the applied magnetic field lead to an increase in the $e-h$ overlap and to a larger exciton binding energy, and would result in a red-shift of the PL peak energy. Of course, again there is a competing effect from the increase in the energy of the $e-h$ non-correlated pair due to the magnetic-field effects on the electron and hole Landau electronic states, and this effect is the dominant one as the value of magnetic field increases, which leads to a blue-shift of the PL peak energy, as expected. In the inset of Fig. 3, the present theoretical results are compared with fair agreement with recent experimental data [11]. Of course, for high values of the applied magnetic field, a reliable calculation should involve a more realistic type of wave function which would appropriately take into account magnetic-field induced anisotropic effects.

Summing up, in the present work we have considered the combined $E-B$ field effects on the excitonic correlated $e-h$ pair for both bulk GaAs and GaAs-$Ga_{1-x}Al_xAs$ QWs. Calculations have been made via a variational procedure in the effective-mass and parabolic-band approximations. The combined effects on the heterostructure properties of the applied crossed electric/magnetic fields together with the direct coupling between the exciton CM and internal exciton motions were appropriately taken into account via a simple parameter representing the distance between the electron and hole magnetic parabolas. Finally, present calculations were shown to lead to the expected behavior for the exciton dispersion in a wide range of the crossed electric/magnetic fields, and theoretical results were found in good agreement with recent experimental measurements by Ashkinadze *et al* [11].

Acknowledgments

The authors would like to thank the Colombian COLCIENCIAS Agency (grant 1115-05-11502), CODI-Univ. de Antioquia, and Brazilian Agencies CNPq, FAPESP, Rede Nacional de Materiais Nanoestruturados/CNPq, and MCT - Millenium Institute for Quantum Computing/MCT for partial financial support. This work was also partially financed by the Excellence Center for Novel Materials ECNM, under Colciencias contract No. 043-2005. CAD and MdDL wish to thank the warm hospitality of the Institute of Physics of UNICAMP, Brazil, where part of this work was performed.

[1] A. Parlangeli, P. C. M. Christianen, J. C. Maan, C. B. Soerensen, and P. E. Lindelof, Phys. Stat. Sol. (a) **178**, 45 (2000); A. Parlangeli, P. C. M. Christianen, J. C. Maan, I. V. Tokatly, C. B. Soerensen, and P. E. Lindelof, Phys. Rev. B **62**, 15323 (2000).
[2] M. Orlita, R. Grill, M. Zvára, G. H. Döhler, S. Malzer, M. Byszewski, and J. Soubusta, Phys. Rev. B **70**, 75309 (2004).
[3] J. Feldmann, G. Peter, E. O. Göbel, P. Dawson, K. Moore, C. Foxon, and R. J. Elliott, Phys. Rev. Lett. **59**, 2337 (1987).
[4] R. Houdré, C. Weisbuch, R. P. Stanley, U. Oesterle, P. Pellandini, and M. Ilegems, Phys. Rev. Lett. **73**, 2043 (1994).
[5] L. P. Gorkov and I. E. Dzyaloshinskii, Soviet Physics JETP **26**, 449 (1968).
[6] M. M. Dignam and J. E. Sipe, Phys. Rev. B **45**, 6819 (1992).
[7] A. B. Dzyubenko and A. L. Yablonskii, Phys. Rev. B **53**, 16355 (1996).
[8] L. V. Butov, A. Zrenner, G. Abstreiter, A. V. Petinova, and K. Eberl, Phys. Rev. B **52**, 12153 (1995); L. V. Butov, A. V. Mintsev, Yu. E. Lozovik, K. L. Campman, and A. C. Gossard, Phys. Rev. B **62**, 1548 (2000).
[9] Kai Chang, J. B. Xia, H. B. Wu, and S. L. Feng, Appl. Phys. Lett. **80**, 1788 (2002).
[10] K. Chang, D. S. Jiang, and J. B. Xia, J. Appl. Phys. **95**, 752 (2004).
[11] B. M. Ashkinadze, E. Linder, E. Cohen, and L. N. Pfeiffer, Phys. Rev. B **71**, 045303 (2005).
[12] E. Reyes-Gómez, L. E. Oliveira, and M. de Dios-Leyva, Phys. Rev. B **71**, 45316 (2005), and references therein.
[13] E. Herbert Li, Physica E **5**, 215 (2000).
[14] B. Gerlach, J. Wüsthoff, M. O. Dzero, and M. A. Smondyrev, Phys. Rev. B **58**, 10568 (1998).
[15] C. A. Duque, L. E. Oliveira, and M. de Dios-Leyva (unpublished).
[16] E. Reyes-Gómez, A. Matos-Abiague, C. A. Perdomo-Leiva, M. de Dios-Leyva, and L. E. Oliveira, Phys. Rev. B **61**, 13104 (2000).